**Advanced Studies in Theoretical Physics**
**Vol. 13, 2019, no. 1, 11 - 22**
**HIKARI Ltd, www.m-hikari.com**
**https://doi.org/10.12988/astp.2019.81249**

# Evaluation of the Difference between a Transient Voltage-Dependent Calcium Conductance and a Stationary Calcium-Inhibited Calcium Conductance in a Mathematical Model of Snail RPa1 Neurons

**Takaaki Shirahata**

Institute of Neuroscience and Kagawa School of Pharmaceutical Sciences,
Tokushima Bunri University, 1314-1 Shido, Sanuki, Kagawa 769-2193, Japan



**Abstract**

A mathematical model of snail RPa1 neurons was previously developed based on the Hodgkin-Huxley formalism. This model is described by a system of nonlinear ordinary differential equations and shows several dynamical states, such as a steady state, a spiking state, and a bursting state, depending on parameter values. The present study performs a numerical simulation analysis of this model and investigates the effect of variation in certain parameters (i.e., transient voltage-dependent calcium conductance and stationary calcium-inhibited calcium conductance) on the model. Variation in the former calcium conductance does not affect the current threshold for the transition from a steady state to a bursting state, whereas variation in the latter calcium conductance affects the current threshold. In addition, a decrease in the former calcium conductance increases bursting frequency, whereas a decrease in the latter calcium conductance decreases bursting frequency. These results will contribute to an in-depth understanding of the difference between two types of calcium conductances in the RPa1 neuron model.

**Mathematics Subject Classification**: 37N25, 92C20

**PACS**: 05.45.-a, 87.19.ll

**Keywords**: Mathematical Model, Numerical Simulation, Snail, Calcium Conductance

## 1 Introduction

Previously, a mathematical model of snail RPa1 neurons was developed based on the Hodgkin-Huxley formulation [1] and described by a system of nonlinear ordinary differential equations (ODEs) [2, 3]. This model can show various types of dynamical states depending on parameter values [2-5]. A previous study indicated that several ionic conductances contained in this model, such as a chemosensitive voltage-activated conductance and a chemosensitive sodium conductance, are important parameters for regulating the dynamical state of the model [3]. Another study also illustrated the time course of calcium currents during a bursting state [2]. Therefore, it is considered that calcium conductances contained in this model are also involved in regulating the dynamical state of the model. As studying membrane conductance is very important [6], it is necessary to investigate, in detail, the effect of variation in calcium conductances on the model. The model includes two types of calcium conductance: transient voltage-dependent calcium conductance and stationary calcium-inhibited calcium conductance. The present study performs a numerical simulation analysis of the RPa1 neuron model and aims to reveal, in detail, the differences between these two calcium conductances.

## 2 The Model

The present study numerically investigated a mathematical model of snail RPa1 neurons that was developed by Komendantov and Kononenko [3]. This model is described by a system of 8-coupled nonlinear ODEs and is based on the concept proposed by Hodgkin and Huxley [1]. State variables of this model are the membrane potential of RPa1 neurons [$V$ (mV)], six ionic current gating variables ($m_B$, $h_B$, $m$, $h$, $n$, and $m_{Ca}$), and the concentration of intracellular calcium {[Ca] (mM)}. The time evolution of these state variables is described by Equations (1) to (8) as shown below:

$$C_m \frac{dV}{dt} = I_{app} - g_{Na(V)} \left( \frac{1}{1+e^{-0.2(V+45)}} \right) (V - V_{Na}) - g_B m_B h_B (V - V_B) - g_{Na} (V - V_{Na}) - g_K (V - V_K) - g_{Na(TTX)} m^3 h (V - V_{Na}) - g_{K(TEA)} n^4 (V - V_K)$$

$$-g_{Ca}{m_{Ca}}^2\left(V-V_{Ca}\right)-g_{CaCa}\left(\frac{1}{1+e^{-0.06(V+45)}}\right)\left(\frac{1}{1+e^{15000([\mathrm{Ca}]-0.00004)}}\right)\left(V-V_{Ca}\right) \quad (1)$$

$$\frac{dm_B}{dt}=\frac{1}{0.05}\left(\frac{1}{1+e^{0.4(V+34)}}-m_B\right) \quad (2)$$

$$\frac{dh_B}{dt}=\frac{1}{1.5}\left(\frac{1}{1+e^{-0.55(V+43)}}-h_B\right) \quad (3)$$

$$\frac{dm}{dt}=\frac{1}{0.0005}\left(\frac{1}{1+e^{-0.4(V+31)}}-m\right) \quad (4)$$

$$\frac{dh}{dt}=\frac{1}{0.01}\left(\frac{1}{1+e^{0.25(V+45)}}-h\right) \quad (5)$$

$$\frac{dn}{dt}=\frac{1}{0.015}\left(\frac{1}{1+e^{-0.18(V+25)}}-n\right) \quad (6)$$

$$\frac{dm_{Ca}}{dt}=\frac{1}{0.01}\left(\frac{1}{1+e^{-0.2V}}-m_{Ca}\right) \quad (7)$$

$$\frac{d[\mathrm{Ca}]}{dt}=rho\left(-\frac{g_{Ca}{m_{Ca}}^2\left(V-V_{Ca}\right)}{2F\left(\frac{4}{3}\pi R^3\right)}-k_s[\mathrm{Ca}]\right) \quad (8)$$

, where $C_m$ (= 0.02 μF) is membrane capacitance; $I_{app}$ is an externally injected current; $g_{Na(V)}$ (= 0.11 μS), $g_{Na}$ (= 0.0231 μS), $g_K$ (= 0.25 μS), $g_B$ (= 0.1650 μS), $g_{Na(TTX)}$ (= 400 μS), $g_{K(TEA)}$ (= 10 μS), $g_{Ca}$, and $g_{CaCa}$ are maximal values of chemosensitive sodium conductance, voltage-independent sodium conductance, voltage-independent potassium conductance, chemosensitive voltage-activated conductance, tetrodotoxin (TTX)-sensitive sodium conductance, tetraethylammonium (TEA)-sensitive potassium conductance, transient voltage-dependent calcium conductance, and stationary calcium-inhibited calcium conductance, respectively; $V_{Na}$ (= 40 mV), $V_K$ (= −70 mV), $V_B$ (= −58 mV), and $V_{Ca}$ (= 150 mV) are reversal potentials of sodium currents, potassium currents, a chemosensitive B current, and calcium currents, respectively; *rho* (= 0.002) is endogenous calcium buffer capacity; $F$ (= 96485 C/mol) is a Faraday constant; $R$ (= 0.1 mm) is cell radius; $k_s$ (= 50 $s^{-1}$) is the rate constant of intracellular calcium uptake by intracellular calcium stores. $I_{app}$, $g_{Ca}$, and $g_{CaCa}$ are control parameters in

the present investigation. $I_{app}$ varied from 0 nA to −1.2 nA. Default values of $g_{Ca}$ and $g_{CaCa}$ were 1.5 μS and 0.02 μS, respectively, and these two parameters varied from 50% to 150% of their default value. A detailed explanation of the above model is provided in [3].

The free and open source software Scilab (http://www.scilab.org/) was used to numerically solve the model equations (1)–(8). Initial conditions were as follows: $V = -42$ mV, $m_B = 0.95$, $h_B = 0.77$, $m = 0.14$, $h = 0.1$, $n = 0.048$, $m_{Ca} = 0.0002$, and $[\mathrm{Ca}] = 13.0 \times 10^{-5}$ mM. The total simulation time was 80 s in all simulations.

## 3 Numerical Results

The present investigation of the snail RPa1 neuron model revealed four dynamical states: a steady state, a regular bursting state, an irregular bursting state, and an irregular spiking state. Examples of the time course of the membrane potential under these four dynamical states are shown in Figure 1: a steady state is shown in Figure 1A, a regular bursting state in Figure 1B, an irregular bursting state in Figure 1C, and an irregular spiking state in Figure 1D.

The effect of variation in $g_{Ca}$ on the model under conditions in which $g_{CaCa}$ was fixed to be a default value and $I_{app}$ was zero was investigated (Figure 2). A decrease in $g_{Ca}$ (i.e., 150%→100%→80%) increased the frequency of regular bursting, and the irregular spiking state was observed at a very small value of $g_{Ca}$ (50%). The effect of variation in $g_{CaCa}$ under conditions in which $g_{Ca}$ was fixed to be a default value and $I_{app}$ was zero on the model was investigated (Figure 3). In contrast to the above result, a decrease in $g_{CaCa}$ (i.e., 150%→100%→80%→50%) decreased the frequency of regular bursting. The effect of simultaneous variation in $g_{Ca}$ and $g_{CaCa}$ on the model under conditions in which $I_{app}$ was zero was investigated (Figure 4). A decrease in both $g_{Ca}$ and $g_{CaCa}$ from 150% to 100% increased the frequency of regular bursting, whereas a decrease in both $g_{Ca}$ and $g_{CaCa}$ from 100% to 50% decreased the frequency of regular bursting.

Next, the effect of variation in $I_{app}$ on the model under certain $g_{Ca}$ and $g_{CaCa}$ conditions was investigated (Figure 5). Changes in $g_{Ca}$ with $g_{CaCa}$ fixed to be a default value did not affect the $I_{app}$ threshold for the transition between a steady state and a regular bursting state (Figure 5A). An increase in $I_{app}$ under conditions in which the value of $g_{Ca}$ was 50% of a default value and the value of $g_{CaCa}$ was a default value transformed the dynamical state of the model from a regular bursting state through an irregular bursting state to an irregular spiking state (Figure 5A). In contrast, an increase in $g_{CaCa}$ with $g_{Ca}$ fixed to be a default value decreased the $I_{app}$ threshold for the transition between a steady state and a regular bursting state (Figure 5B); the effect of an increase in both $g_{Ca}$ and $g_{CaCa}$ simultaneously was the same (Figure 5C).

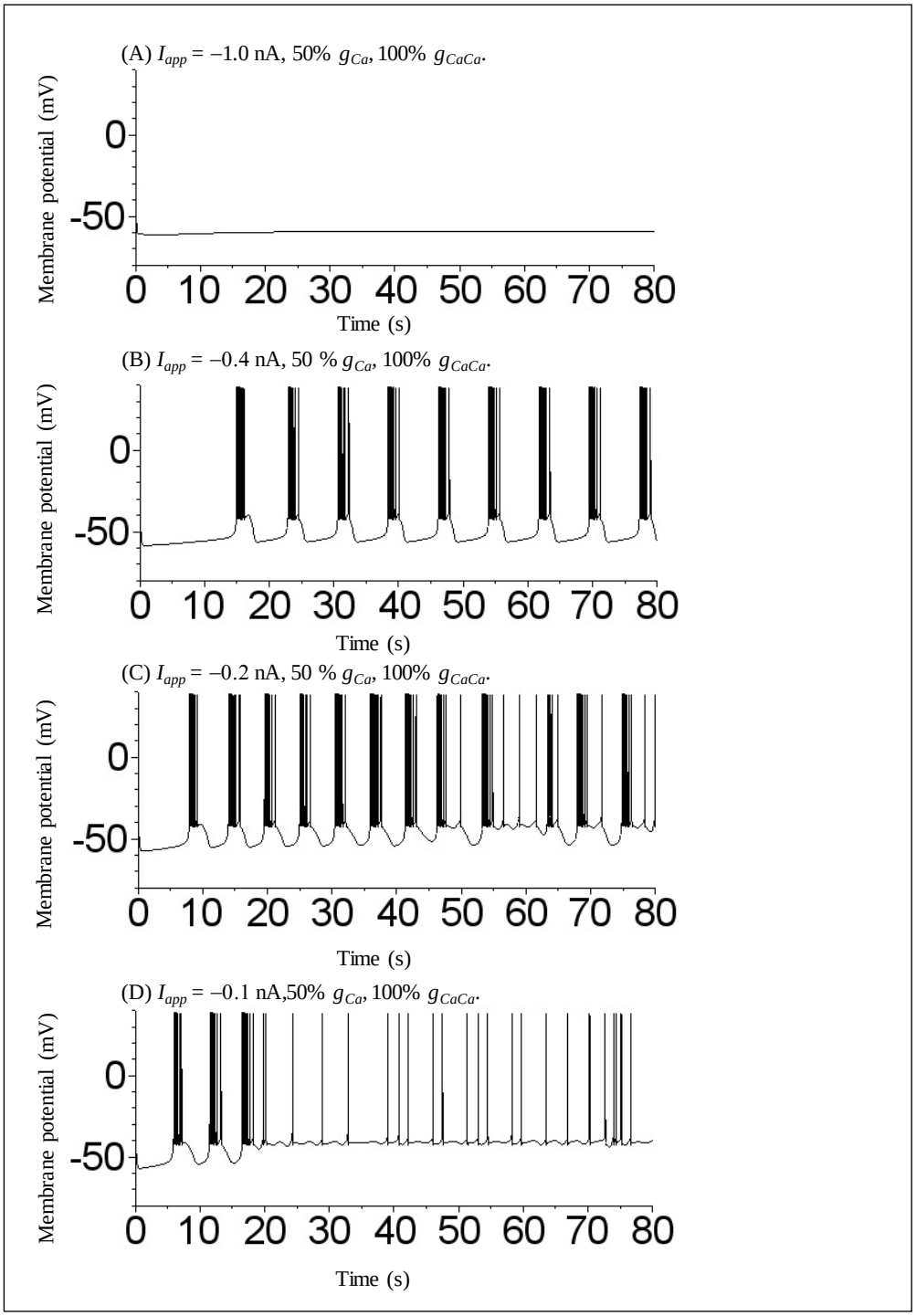


**Figure 1**. Time courses of the membrane potential of the RPa1 neuron model. (A) $I_{app}$ = −1.0 nA, 50% $g_{Ca}$, 100% $g_{CaCa}$, (B) $I_{app}$ = −0.4 nA, 50% $g_{Ca}$, 100% $g_{CaCa}$, (C) $I_{app}$ = −0.2 nA, 50% $g_{Ca}$, 100% $g_{CaCa}$, (D) $I_{app}$ = −0.1 nA, 50% $g_{Ca}$, 100% $g_{CaCa}$.

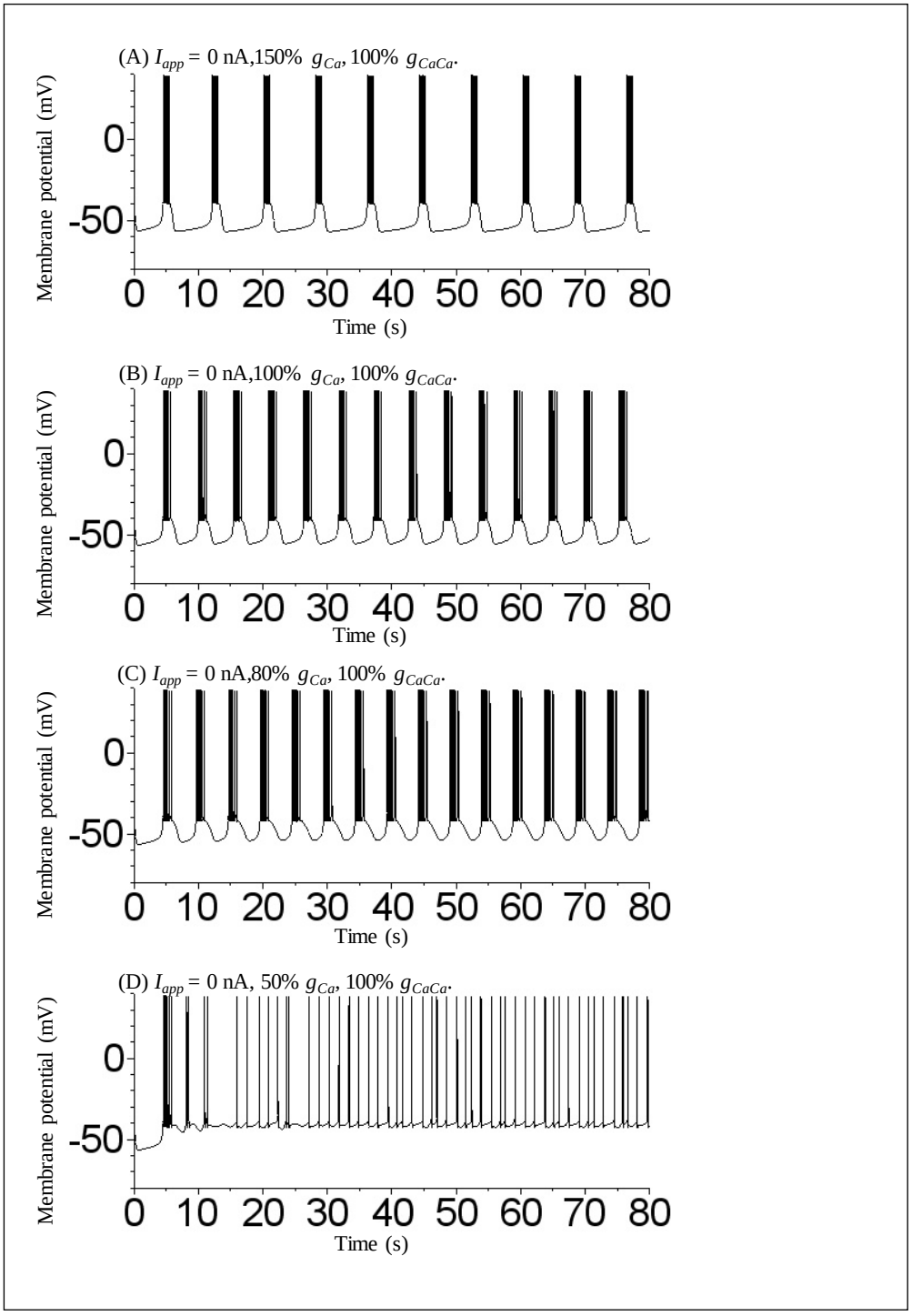


**Figure 2**. Time courses of the membrane potential of the RPa1 neuron model. (A) $I_{app}$ = 0 nA, 150% $g_{Ca}$, 100% $g_{CaCa}$, (B) $I_{app}$ = 0 nA, 100% $g_{Ca}$, 100% $g_{CaCa}$, (C) $I_{app}$ = 0 nA, 80% $g_{Ca}$, 100% $g_{CaCa}$, (D) $I_{app}$ = 0 nA, 50% $g_{Ca}$, 100% $g_{CaCa}$.

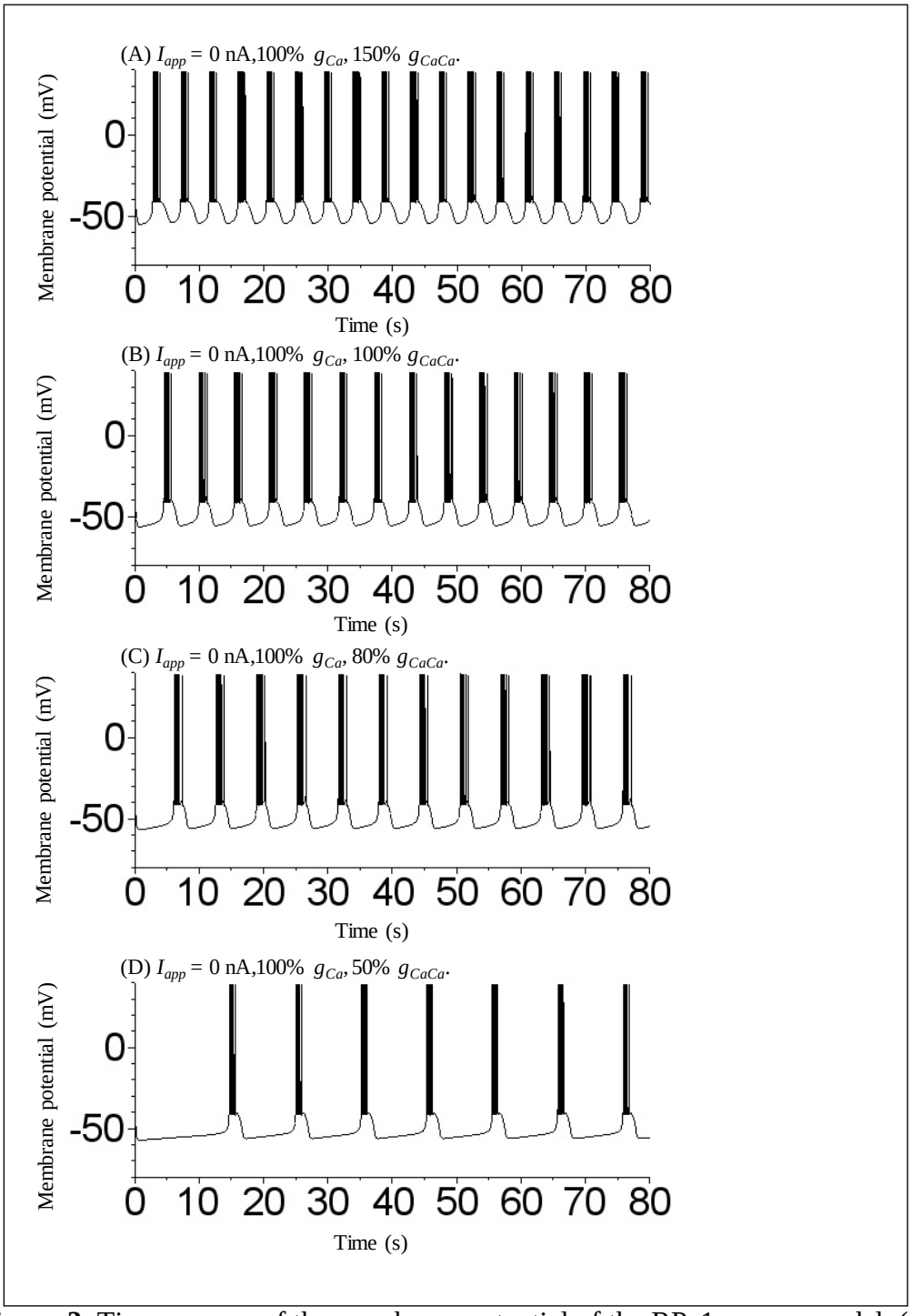


**Figure 3**. Time courses of the membrane potential of the RPa1 neuron model. (A) $I_{app}$ = 0 nA, 100% $g_{Ca}$, 150% $g_{CaCa}$, (B) $I_{app}$ = 0 nA, 100% $g_{Ca}$, 100% $g_{CaCa}$, (C) $I_{app}$ = 0 nA, 100% $g_{Ca}$, 80% $g_{CaCa}$, (D) $I_{app}$ = 0 nA, 100% $g_{Ca}$, 50% $g_{CaCa}$.

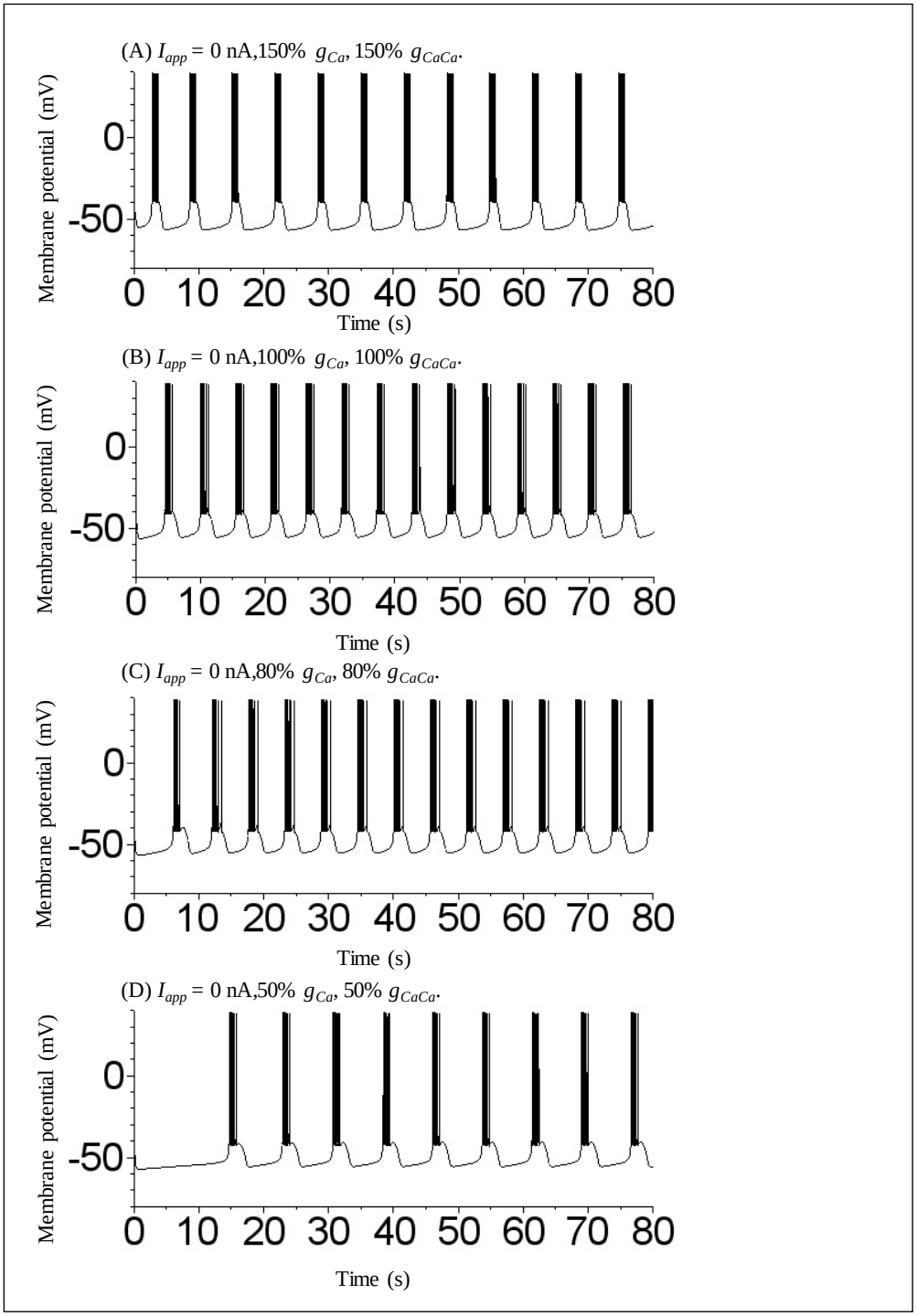


**Figure 4**. Time courses of the membrane potential of the RPa1 neuron model. (A) $I_{app}$ = 0 nA, 150% $g_{Ca}$, 150% $g_{CaCa}$, (B) $I_{app}$ = 0 nA, 100% $g_{Ca}$, 100% $g_{CaCa}$, (C) $I_{app}$ = 0 nA, 80% $g_{Ca}$, 80% $g_{CaCa}$, (D) $I_{app}$ = 0 nA, 50% $g_{Ca}$, 50% $g_{CaCa}$.

△: steady state,
●: regular bursting state,
◎: irregular bursting state,
○: irregular spiking state.

| | $I_{app}$ (nA) | | | | | | | | | | | | |
|---|---|---|---|---|---|---|---|---|---|---|---|---|---|
| (A) | -1.2 | -1.1 | -1.0 | -0.9 | -0.8 | -0.7 | -0.6 | -0.5 | -0.4 | -0.3 | -0.2 | -0.1 | 0.0 |
| 50% $g_{Ca}$, 100% $g_{CaCa}$ | △ | △ | △ | △ | △ | △ | ● | ● | ● | ● | ◎ | ○ | ○ |
| 100% $g_{Ca}$, 100% $g_{CaCa}$ | △ | △ | △ | △ | △ | △ | ● | ● | ● | ● | ● | ● | ● |
| 150% $g_{Ca}$, 100% $g_{CaCa}$ | △ | △ | △ | △ | △ | △ | ● | ● | ● | ● | ● | ● | ● |

| | $I_{app}$ (nA) | | | | | | | | | | | | |
|---|---|---|---|---|---|---|---|---|---|---|---|---|---|
| (B) | -1.2 | -1.1 | -1.0 | -0.9 | -0.8 | -0.7 | -0.6 | -0.5 | -0.4 | -0.3 | -0.2 | -0.1 | 0.0 |
| 100% $g_{Ca}$, 50% $g_{CaCa}$ | △ | △ | △ | △ | △ | △ | △ | △ | △ | △ | △ | ● | ● |
| 100% $g_{Ca}$, 100% $g_{CaCa}$ | △ | △ | △ | △ | △ | △ | ● | ● | ● | ● | ● | ● | ● |
| 100% $g_{Ca}$, 150% $g_{CaCa}$ | △ | △ | ● | ● | ● | ● | ● | ● | ● | ● | ● | ● | ● |

| | $I_{app}$ (nA) | | | | | | | | | | | | |
|---|---|---|---|---|---|---|---|---|---|---|---|---|---|
| (C) | -1.2 | -1.1 | -1.0 | -0.9 | -0.8 | -0.7 | -0.6 | -0.5 | -0.4 | -0.3 | -0.2 | -0.1 | 0.0 |
| 50% $g_{Ca}$, 50% $g_{CaCa}$ | △ | △ | △ | △ | △ | △ | △ | △ | △ | △ | △ | ● | ● |
| 100% $g_{Ca}$, 100% $g_{CaCa}$ | △ | △ | △ | △ | △ | △ | ● | ● | ● | ● | ● | ● | ● |
| 150% $g_{Ca}$, 150% $g_{CaCa}$ | △ | △ | ● | ● | ● | ● | ● | ● | ● | ● | ● | ● | ● |

**Figure 5**. Dependence of the dynamical state of the RPa1 neuron model on $I_{app}$, $g_{Ca}$, and $g_{CaCa}$. (A) Dependence on $I_{app}$ and $g_{Ca}$. (B) Dependence on $I_{app}$ and $g_{CaCa}$. (C) Dependence on $I_{app}$ and two calcium conductances. △ indicates a steady state; ● indicates a regular bursting state; ◎ indicates an irregular bursting state; ○ indicates an irregular spiking state.

## 4 Discussion

The present investigation revealed the relationship between parameter variations and the transition between different dynamical states. In particular, the current threshold for the transition from a steady state to a regular bursting state is sensitive to variation in a stationary calcium-inhibited calcium conductance but not to variation in a transient voltage-dependent calcium conductance (Figure 5). Mathematical modeling studies of other neurons also revealed the relationship between parameter variations and dynamical state changes of the model [7-10]. However, the RPa1 neuron model in the present study is more useful for studying a bursting state than the methods of these four previous studies, in which a bursting state was not observed.

The effect of a decrease in calcium conductance on the RPa1 neuron model was investigated previously [11]. This previous study shows that simultaneously setting two types of calcium conductance values to zero induces a decrease in bursting frequency. A similar conclusion was derived in the present study: a decrease in two types of calcium conductances simultaneously induces a decrease in bursting frequency (Figure 4B, 4C, and 4D). However, the previous study did not clarify the effect of varying each calcium conductance independently on the model [11]. An interesting novel finding of the present study is that two types of calcium conductances have the opposite effect on bursting frequency: a decrease in transient voltage-dependent calcium conductance induces an increase in bursting frequency (Figure 2A, 2B, and 2C), whereas a decrease in stationary calcium-inhibited calcium conductance induces a decrease in bursting frequency (Figure 3A, 3B, 3C, and 3D)

## 5 Conclusion

The present study performed a numerical simulation analysis of a mathematical model of snail RPa1 neurons and investigated the effect of variation in different types of calcium conductances on the model in more detail than previous studies. The present results contribute to an in-depth understanding of the difference between transient voltage-dependent calcium conductance and stationary calcium-inhibited calcium conductance in the RPa1 neuron model.

**Acknowledgements.** The author would like to thank Enago (www.enago.jp) for the English language review.

## References

[1] A. L. Hodgkin and A. F. Huxley, A quantitative description of membrane current and its application to conduction and excitation in nerve, *Journal of Physiology*, **117** (1952), no. 4, 500-544.

https://doi.org/10.1113/jphysiol.1952.sp004764

[2] N. M. Berezetskaya, V. N. Kharkyanen and N. I. Kononenko, Mathematical model of pacemaker activity in bursting neurons of snail, *Helix pomatia*, *Journal of Theoretical Biology*, **183** (1996), no. 2, 207-218. https://doi.org/10.1006/jtbi.1996.0214

[3] A. O. Komendantov and N. I. Kononenko, Deterministic chaos in mathematical model of pacemaker activity in bursting neurons of snail, *Helix pomatia*, *Journal of Theoretical Biology*, **183** (1996), no. 2, 219-230. https://doi.org/10.1006/jtbi.1996.0215

[4] T. Shirahata, Novel types of bistability in a model of a bursting pacemaker neuron RPa1 from the snail, *Helix pomatia*, *Acta Biologica Hungarica*, **64** (2013), no. 1, 131-135. https://doi.org/10.1556/abiol.64.2013.1.12

[5] T. Shirahata, Numerical simulation of bistability between regular bursting and chaotic spiking in a mathematical model of snail neurons, *International Journal of Theoretical and Mathematical Physics*, **5** (2015), 145-150.

[6] M. Ashrafuzzaman and J. Tuszynski, *Membrane Biophysics, Biological and Medical Physics, Biomedical Engineering*, Heidelberg, Springer, 2012.

[7] G. Drion, L. Massotte, R. Sepulchre and V. Seutin, How modeling can reconcile apparently discrepant experimental results: The case of pacemaking in dopaminergic neurons, *PLoS Computational Biology*, **7** (2011), no. 5, e1002050. https://doi.org/10.1371/journal.pcbi.1002050

[8] T. Shirahata, Evaluating Bistability in a Mathematical Model of Circadian Pacemaker Neurons, *International Journal of Theoretical and Mathematical Physics*, **6** (2016), 99-103.

[9] T. Shirahata, A Mathematical Modeling Study of Dopaminergic Retinal Neurons under Hyperpolarized Conditions, *International Journal of Theoretical and Mathematical Physics*, **7** (2017), 4-8.

[10] T. Shirahata, Numerical Study of the Bistability of a Mathematical Model of Neocortical Pyramidal Neurons, *Applied Mathematical Sciences*, **12** (2018), 105-114. https://doi.org/10.12988/ams.2018.712364

[11] E. E. Saftenku, Simulation of bursting activity in the *Helix* RPA1 neuron: Role of calcium ions, *Neurophysiology*, **26** (1994), no. 5, 307-314. https://doi.org/10.1007/bf01058510

**Received: January 3, 2019; Published: January 22, 2019**